

# ASSOCIATION OF FLAME-OSCILLATION FREQUENCY UNDER CROSS WIND DIFFUSION

Bo Lou<sup>1\*</sup>, Eric Hu<sup>2</sup>, Ye Wang<sup>1</sup>

(1. School of Electric Power, South China University of Technology, Guangzhou, Guangdong Province, China,; 2. School of Mechanical Engineering, the University of Adelaide, Adelaide, Australia)

**Abstract:** Turbulent flame-oscillation frequency and combustion efficiency are the important parameters in combustion. It is a useful study to judge combustion efficiency by intuitive flame frequency. Based on a combustion wind tunnel experimental setup, the variation law of combustion flame-oscillation frequency and combustion efficiency using external wind speeds was studied via the color flames image sequence of oil pan combustion and flue gas composition. The oscillation frequency was calculated with the upper edge of the fire plume which recorded flame image sequence using a high-speed video, combined the MATLAB image processing technique. The combustion efficiency was calculated combined with the C and H element mass of the liquid fuel in the oil pool and CO<sub>2</sub> and H<sub>2</sub>O concentrations in the flue gas. The results show that the oscillation frequency of the flame revealed a tendency to increase followed by a decrease with increasing wind speed, while the overall trend of combustion efficiency increased first and then decreased. The combustion efficiency could be judged by observing the oscillation frequency of the flame image. In addition, the combustion efficiency may ensure in right way when the turbulence oscillation frequency of the oil pan flame ranged between 15 HZ and 18 HZ.

**Keywords:** cross wind; combustion characteristics; flame-oscillation frequency; combustion efficiency; flame image

## 1. Introduction

Flame oscillation generally represents the instability of a flame, low oscillation frequency of the flame occur in the vicinity of the boundary between the outer flame and the surrounding air stream[1],and it can reflect the specific characteristics of combustion[2]. The intrinsic cause of flame oscillation is the result of vortex movement within the flame plume, which is the macroscopic representation of the small-size structure within the flame. In 1984, Zukoski *et al.* [3] reported that the flame diameter at the top of the sump periodically shrank to form a regular flame cluster, while the flame showed periodic oscillations. It was suggested that the oscillation was mainly caused by the flame in the thermal buoyancy of the surrounding air, which caused the periodically generated vortex, transmission, and shedding. Cetegen *et al.* [4] suggested an empirical relationship for predicting the flame-oscillation frequency, which showed that the oscillation frequency of the oil pan has a relation with dimensionless Froude number  $Fr$ , and furthermore reported that the fuel outlet flow rate and the heat release rate were not significantly related to the pulsation frequency for a fixed-diameter flame.

In generally, most studies of the flame-oscillation frequency are concentrated in the windless conditions. However, cross wind combustion is a common form of combustion, which will change the flame shape and flame oscillation frequency. Atzler *et al.*[5] studied flame oscillations and burning rates with globally homogeneous two phase mixtures, the results show association between the flame burning rates and the oscillation frequency in premixed flames. Kelso *et al.* [6] Fric and Roshko

41 [7]experimentally described the shear-layer vortices, the horseshoe vortices, the counter-rotating  
42 vortex pair, and the wake vortices of pool fire under the action of cross wind, thus revealing the  
43 intrinsic mechanism of flame-oscillation from a microscopic point of view.

44 There is a certain relationship between cross wind and fuel combustion efficiency. Tsue *et al.*[8]  
45 proposed a test method to measure the efficiency of jet diffusion flame combustion under cross wind  
46 conditions and found that lateral airflow reduced combustion efficiency. Bourguignon *et al.* [9] studied  
47 the effects of external wind speed, fuel flow rate, and fuel composition on combustion efficiency in  
48 1999, using a closed-loop wind tunnel system. In their experiment, the combustion efficiency of the  
49 fuel was calculated via carbon atom conservation under the assumption that the combustion products  
50 are both gas and without carbon black. Gogolek *et al.*[10] focused on the effects of wind flow patterns  
51 (laminar flow and turbulence) on combustion efficiency. Johnson *et al.*[11-12] studied the effect of  
52 fuel type, jet exit velocities, and nozzle type on combustion efficiency under the action of cross wind,  
53 and presented an empirical model to characterize fuel combustion efficiency.

54 Buoyancy and momentum are two major driving forces that affect the behavior of diffusion  
55 flames, Fang *et al* [13] investigates both buoyancy (B)- and momentum (M)-driven methane laminar  
56 diffusion flame shapes with the different fuel mass flow rate and under the ambient pressure range of  
57 0.45 - 1.00 atm. Radiation, and the oscillation frequency of the observed flame flickering motions are  
58 determined and analyzed to reveal the effects of pressure on the two dominating mechanisms of flames.  
59 Ping *et al* [14]presents an experimental investigation on mass burning rate and flame geometry  
60 characteristics of crude oil boilover fire under cross air flows, whose cross air flow speed ranges from  
61 0 to 1.5 m/s, and the results show that the response of steady mass burning rate to cross air flow  
62 velocity showed a non-monotonic trend. Cross wind has a great influence on the combustion oscillation  
63 frequency and combustion efficiency. Therefore, a quantitative analysis of the combustion oscillation  
64 law and the relationship between the oscillation frequency and the combustion efficiency of the flame  
65 is vitally important to reveal the combustion mechanism and its application, something that previous  
66 studies in this area lacked.

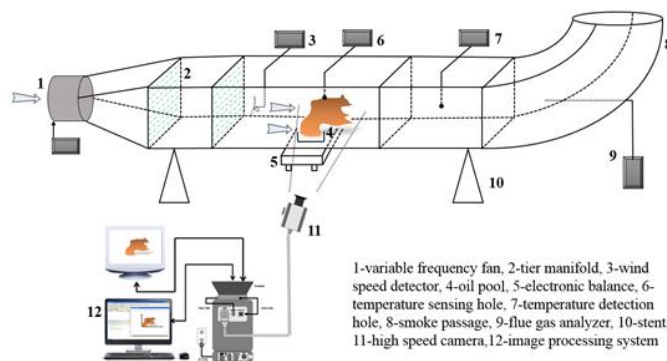
67 The experimental data of Flame-Oscillation Frequency were obtained by using three techniques  
68 namely, pressure fluctuation, measurements, thermal imaging and high-speed video photography[15].  
69 Pressure fluctuation measurement in flame need a high-precision measuring instrument and usually is  
70 difficulty, high-speed video photography is actually easier to observe the fluctuations with the thermal  
71 contour map. In this study, the flame oscillation frequency under the action of the cross wind was  
72 obtained via a combustion wind tunnel experiment and high-speed video photography. Furthermore, a  
73 quantitative analysis of combustion efficiency was conducted considering changes in wind speed. This  
74 study is to correlate the frequency of combustion flame with combustion efficiency, which will be  
75 helpful for judging combustion efficiency by flame frequency in the future.

## 76 **2. Experimental setuo and method**

77 The experiments were conducted in a combustion wind tunnel with an internal dimension of 5000  
78 mm (length) × 300 mm (width) × 500 mm (height). The wind tunnel was divided into a front section, a  
79 combustion section, and a latter part of the three parts, of which the front length was 1800 mm. The  
80 front section of the port was equipped with a variable frequency fan, which has an adjustable  
81 frequency range of 0-50 HZ; a two-tier manifold was located behind the fan exhaust to ensure uniform

82 airflow into the combustion section, and following the flow of the network set was a wind speed  
 83 detection hole. The combustion section length was 1200 mm, the observation surface was covered  
 84 with 5 mm thick tempered glass, the other surfaces were covered with 5 mm steel plates, and all gaps  
 85 were filled with sealant. At the top of the combustion section, a temperature sensing hole enabled  
 86 measurement of the flame temperature, and the bottom of the center contained fuel for the light diesel  
 87 oil pool with a size of 120 mm (length)  $\times$  50 mm (width)  $\times$  50 mm (height). The cetane number of  
 88 diesel oil is 51, its carbon mass fraction is 88.7%, the hydrogen is 11.3%, and the low calorific value is  
 89 42.6MJ/kg. Situated underneath the oil tank was an electronic balance (mass accuracy 0.1 g, sampling  
 90 frequency 2 Hz), used to measure the changes of fuel mass during the combustion process. A color  
 91 high-speed camera (Canadian NORPIX, model FR340-10G) was placed on the front of the  
 92 combustion zone, recording the burning process of the oil mist at 150 frames per second (FPS) or  
 93 other at different wind speeds to obtain the flame image sequence as a function of wind speed. At the  
 94 top of latter section, several temperature detection holes were set to measure flue gas temperature. In  
 95 addition, a German testo340 flue gas analyzer was installed at the end of the exhaust channel to  
 96 measure the O<sub>2</sub>, CO, and C<sub>n</sub>H<sub>m</sub> concentrations in the flue gas. The experimental setup and  
 97 measurement arrangement are shown in Fig. 1.

98



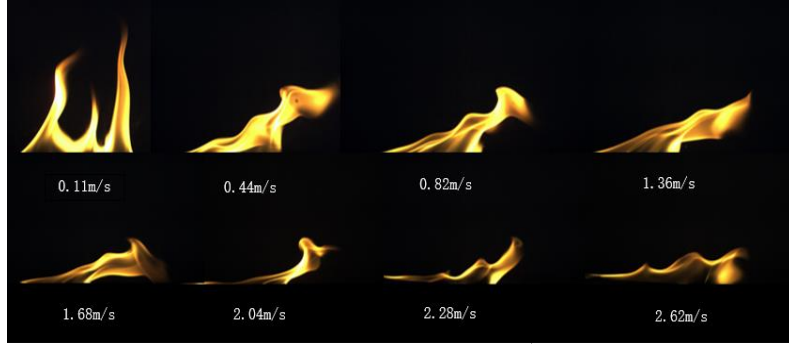
99

Fig.1 Experimental system diagram

100 In the preliminary experiment, it is found that the fan frequency was below 2 Hz will result to  
 101 wind speed below 0.11 m/s, the flame did not have a significant impact, and the fan frequency was  
 102 higher than 22 Hz, the oil tank was close to the bottom of the wind tunnel which also made high-speed  
 103 camera recording image of poor quality. Therefore, the experimental fan frequency was set to 2-22 Hz  
 104 in this study. According to the results of the combustion section wind speed measuring instrument, the  
 105 relationship between frequency verses with wind speed of the inverter fan was study in preparatory  
 106 experiment.

107 The burning process of the flame at different wind speeds were recorded with a high-speed  
 108 camera and then were transmitted to a batch processor, which used self-contained software to obtain a  
 109 flame image sequence at different wind speeds. Fig. 2 shows the combustion flame images at several  
 110 different wind speeds.

111 The flame image sequence in Fig. 2 shows that as the wind speed increases, the angle of  
 112 the flame that deviates from the vertical direction increased [16], and the visible area of the  
 113 flame plume decreased [17].



114 Fig.2 Burning flame images at different wind speeds

### 115 3. Experimental results and analysis

116 Unlike a stationary fire, the flames of combustion are mainly affected by buoyancy in vertical  
 117 direction, and the combustion under cross wind is also affected by the horizontal force.

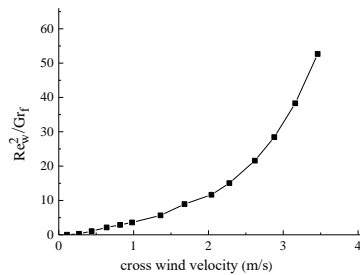
#### 118 3.1. Effect of cross wind on the flame

119 To investigate the action of jet diffuse flames under the action of cross wind, Gollahalli *et al.* [18]  
 120 used the momentum flux ratio of the external wind speed and the jet exit speed to measure the effect of  
 121 the interaction on the combustion. The fuel outlet speed of the oil pool flame was difficult to measure,  
 122 however, an accurate R value could not be obtained. Maughan *et al.* [19] analyzed the heat transfer of  
 123 the mixed convection between the flame and the air under the action of external airflow, using  
 124  $Gr/Re^2$  as the criterion to judge the degree of natural convection. Using a similarity analysis method  
 125 reveals that the Gr number contains the ratio of the buoyant force to the viscous force. Re is the ratio  
 126 of inertial force to viscous force, then the ratio of buoyancy to inertia can be obtained from Gr and Re.  
 127 To highlight the role of the wind, this study applied  $Re_w^2/Gr_f$  to analyze the extent of the impact of  
 128 the wind on the combustion of the oil pan. The formula is as follows:

$$129 \frac{Re_w^2}{Gr_f} = \frac{u_w^2 l_w^2}{v_w^2} * \frac{v_f^2}{g \alpha_V \Delta T l_w^3} \quad (1)$$

130 Following the previous principles [19], when  $Re_w^2/Gr_f < 0.1$ , flame is mainly influenced by  
 131 buoyancy, and  $0.1 \leq Re_w^2/Gr_f \leq 10$  is the mixing stage. when  $Re_w^2/Gr_f > 10$ , the influence of cross  
 132 wind on the flame is dominant. Fig. 3 shows the variation curve of  $Re_w^2/Gr_f$  in the range of  
 133 experimental wind.

134



135

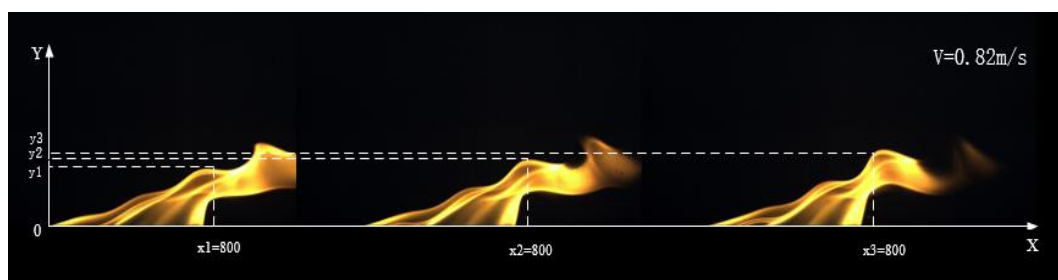
136 Fig.3  $Re_w^2/Gr_f$  change curve in the different wind speeds

137 Fig. 3 and the flame image in Fig. 2 show that when the wind speed  $0 < u_w < 0.44 \text{ m/s}$ ,  
 138 the  $Re_w^2/Gr_f < 0.1$ , and the compulsory force from the cross wind speed may be negligible.  
 139 Then, The oil combustion flame is mainly affected by buoyancy in the vertical direction. When  
 140  $0.44 \text{ m/s} < u_w < 1.68 \text{ m/s}$  and  $0.1 \leq Re_w^2/Gr_f \leq 10$ , the combustion is in the mixed phase. The buoyancy  
 141 force and the inertial force formed by the external wind speed interact with each other, and the upper  
 142 edge of the flame shows obvious fluctuation. When  $u_w > 1.68 \text{ m/s}$  and  $Re_w^2/Gr_f > 10$ , the effect of  
 143 forced cross flow wind to fire becomes dominant and the flame remains close to the bottom of the  
 144 wind tunnel.

### 145 3.2. Turbulent fluctuation of flame

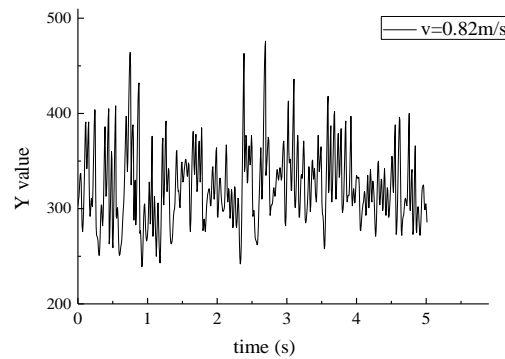
146 The pool flame exhibited periodic shrinkage and expansion as one of the most striking phenomena  
 147 observed in the experiment. The contraction of the flame cross-section led to an increase in height and  
 148 a decrease in cross-section expansion, which is due to the entrainment effect in the formation of vortex  
 149 flame propagating upward and shedding [20]. In the absence of wind conditions, the oscillation of the  
 150 flame can be described by a periodic variation of the flame height in the vertical direction. Under the  
 151 action of wind, the influence of the external air force and its own buoyancy not only changes the shape  
 152 of the flame (including height, area, and tilt angle) [20-21], but also the vortex formed at the periphery  
 153 of the flame. The shear layer vortex generated by the cross wind was mainly caused by the formation  
 154 of Kelvin-Helmholtz instability [7], *i.e.*, when air and flame of these two different density fluids met  
 155 on the interface, the difference of speed caused a pressure difference, then forming torque and  
 156 growing into a vortex. The eddy current near the fuel side moves along the direction of the plume,  
 157 which merged with the downstream vortices to form a certain period of turbulent flame pulsation.

158 The fluctuation of the upper edge of the flame was observed in the flame image, which showed the  
 159 periodic turbulence pulsation formed by the shear layer vortex. The turbulence oscillation frequency  
 160 could be obtained by tracking the average cycle time of the upper edge of the flame. Each image in  
 161 MATLAB was composed of a two-dimensional array, and its value representing the pixel value.  
 162 Selection of flame image sequences of a time interval, and the lower left corner of the numerical  
 163 position as the origin of coordinates, then the number of horizontal numerical in the array is the  
 164 abscissa  $x$ , and the number of vertical numerical is the ordinate  $Y$ . Extracting the  $Y$ -value of the  
 165 upper edge of the flame in each image  $x = 800$ , Fig.4 can be drawn. Because of the same overall  
 166 oscillation frequency, the flame at other locations is also acceptable. For the same wind speed, the  
 167 upper edge of the flame fluctuated over time, resulting in a change in height ( $Y$ -value) of the upper  
 168 edge of the flame at a fixed abscissa, which reveals the fluctuation period of the upper edge of the  
 169 flame at this wind speed. Three flame images in fig. 4 are shown with wind speed  $v = 0.82 \text{ m/s}$ , the  
 170 time interval between each two images was  $0.016 \text{ s}$ , and the corresponding  $y_1, y_2,$  and  $y_3$  at  $x = 800$   
 171 were the heights of the upper edge of the flame.



173 Fig.4 The height of upper edge of the flame at different times in the same wind speed  $v = 0.82$   
174 m/s,  $X=800$ , time interval 0.016 s.

175 Selecting the wind speed  $u_w = 0.82$  m/s and setting the high-speed camera to 150 FPS , it may  
176 produced 750 flame image sequences (*i.e.*, the burning time of 5 sec). The time-varying law of Y  
177 value of flame upper edge at  $x=800$  in image sequence was obtained via using MATLAB. The result  
178 was shown in Fig. 5.



179

180 Fig.5 The time-varying law of the upper edge of the flame at  $x = 800$ , in a flame image with a  
181 wind speed  $v = 0.82$  m/s ,the burning time of 5 sec, setting high-speed camera 150 FPS

182 In Fig. 5, the mean time interval of the adjacent peak points was calculated to obtain the average  
183 fluctuation period of the curve. At the same wind speed, the experiment was repeated 5 times under  
184 the condition of  $u_w = 0.82$  m/s, and then verage the the flame-oscillation frequency. Next, using the  
185 same method at different wind speeds reveals the change rule between flame-oscillation frequency and  
186 cross wind speed.

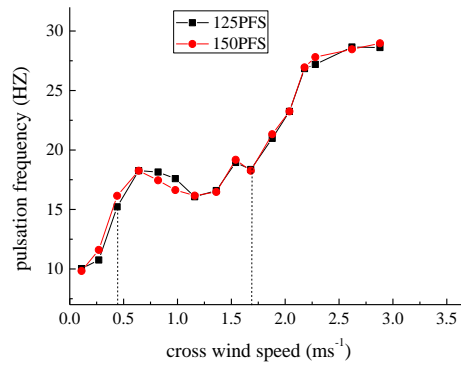
187 Fig. 6 shows the variation of the flame-oscillation frequency with the cross wind speed when the  
188 frame rates were 150 FPS and 125 FPS. Under the condition of different frame rates, the trend was  
189 very close after the wind speed increased, the wind turbulence speed was slightly different at 1.0 m/s.  
190 So, The frequency of flame oscillation has little correlation with frame rate of high-speed camera. In  
191 this study results are based on the high-speed video photography of 150 FPS.

192 When  $0.11\text{m/s} < u_w < 0.64\text{m/s}$ , oscillation frequency increased as wind speed increased, and the  
193 oscillation frequency reached a maximum value. The flame-oscillation frequency decreased ,when  
194  $0.64 < u_w < 1.36$  m/s. Then the turbulence increased with increasing wind speed after  $u_w > 1.36$   
195 m/s. It can be seen that in the range of wind speed, the oscillation frequency of the flame first  
196 increased, then decreased, and then increased again.

197 The range of  $Re_w^2/Gr_f$  in Fig.3 shows that when the wind speed was  $0.11\text{m/s} < u_w < 0.44$  m/s,  
198 then  $Re_w^2/Gr_f < 0.1$  ,the influence of wind was weak, and the flame was mainly affected by the  
199 buoyancy. However, increasing wind speed exacerbates the perturbation between ambient air and  
200 flame, the acceleration and extinction of the vortex in the upper edge of the flame increased the  
201 turbulence oscillation frequency of the flame. When  $0.44 \text{ m/s} \leq u_w \leq 1.68 \text{ m/s}$ ,  $0.1 \leq Re_w^2/Gr_f \leq 10$ ,  
202 the interaction between external airflow and buoyancy force changed the force on the flame plume  
203 during the mixing stage. At this time, the oscillation frequency fluctuated, it remained in the range of

204 15 Hz - 18 Hz. As the wind speed increased (when  $u_w > 1.68$  m/s,  $Re_w^2/Gr_f \geq 10$ ), the external wind  
 205 extracted a large amount of heat, then reduced flame temperature and buoyancy. The force of the wind  
 206 swept is on the dominant position and the difference enlarged between the two forces of buoyancy and  
 207 cross wind ,then make a horizontal tilt of the flame (see Fig. 2) and the flame-oscillation frequency  
 208 continued to increase .

209

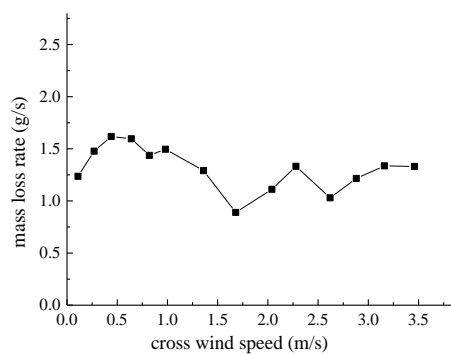


210

211 Fig.6 Curve diagram of flame oscillation frequency versus wind speed at 150FPS and 125FPS

212 **3.3. Combustion efficiency**

213 In the diffusion combustion process, the combustion rate of liquid fuel was determined by the heat  
 214 transfer from the surrounding high temperature flue gas to the fuel. High temperature flue gas fed the  
 215 heat into the liquid fuel via radiation, heat conduction, and convection to evaporate the liquid fuel into  
 216 combustible gas, so that the amount of liquid fuel heat absorption directly determined the degree of  
 217 flame burning. However, under the effect of cross wind, the burning process becomes more  
 218 complicated due to the influence of heat transfer between oil and wind. The calculation of combustion  
 219 efficiency in the study was obtained by measuring the mass loss rate of the liquid fuel in measurement  
 220 interval, specifically by measuring the mass-change curve of the oil tank using the electronic balance  
 221 below the oil pool.the mass loss rate of the light diesel oil were gotten in different cross wing speed,  
 222 The result was shown in Fig. 7.



223

224 Fig.7 Variation curve of fuel mass loss rate at different wind speeds

225 Fig. 7 shows that the mass loss rate of the fuel increased with increasing wind speed when 0.11

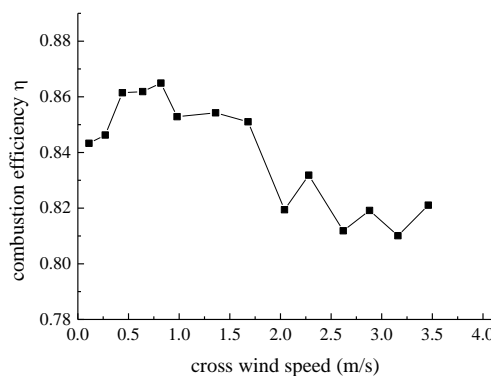
226 m/s <  $u_w$  < 0.44 m/s. Wind accelerated the gasification rate of the oil in the oil pool, made  
 227 combustion intensify and the temperature increase. When 0.44 m/s <  $u_w$  < 1.68 m/s, the mass loss  
 228 rate showed a downward trend. The combustion rate of the liquid fuel depended mainly on the amount  
 229 of heat absorbed by the fuel, which was decided by on the temperature difference between fuel and oil  
 230 pool wall. Hu *et al.* [22] showed that with increasing wind speed, the flame tilted to the plane,  
 231 resulting in a small fuel view surface, greatly reducing fuel surface of the received heat. While the oil  
 232 pool surface temperature reduces, caused a decrease of fuel gasification rate and led to a reduction in  
 233 the mass loss rate of the fuel. When the cross flow speed  $u_w$  > 1.68 m/s, flame caused severe tilt and  
 234 even became parallel with the bottom of the wind tunnel (Fig. 2). The wall surface of the oil pool was  
 235 directly heated by heat convection and heat radiation of the fire , and increasing the mass loss rate[23].

236 The combustion efficiency was defined as the ratio of actual heat, released during the burning  
 237 process, to its complete combustion. The C element in the fuel was completely burned to produce CO<sub>2</sub>  
 238 gas, while the H element burned into H<sub>2</sub>O. The CO<sub>2</sub> and H<sub>2</sub>O concentrations in the flue gas after  
 239 complete combustion can be calculated by measuring the C and H element mass of the liquid fuel in  
 240 the oil pool. However, during the actual process, the calculation of combustion efficiency requires the  
 241 CO and CnHm concentrations in flue gas owing to incomplete combustion. The combustion efficiency  
 242 can be expressed as:

243

$$244 \quad \eta = 1 - \frac{\text{CO and CnHm concentrations in flue gas} \cdot \text{Volume flow}}{\text{The amount of CO}_2 \text{ and H}_2\text{O produced by complete combustion per unit time}} \quad (2)$$

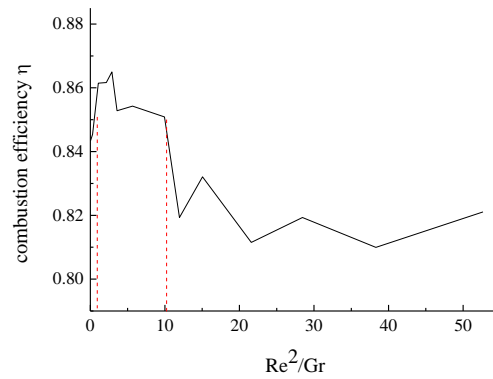
245 CO concentrations and CnHm concentrations were measured with the on-line flue gas analyzer  
 246 (Testo 350, TestoSE & Co. KGaA,Germany).The change in combustion efficiency at different wind  
 247 speeds was calculated according to the previous rate of fuel mass loss and formula (2), the results were  
 248 shown in Fig. 8.



249

250 Fig.8 Curve of combustion efficiency at different wind speeds





251

252

Fig.9 Combustion efficiency changes with  $Re_w^2/Gr_f$

253

254

255

256

257

258

259

260

Fig. 8 shows that the overall trend of combustion efficiency first increased and then decreased as the lateral wind speed increased. When  $0.11 < u_w < 0.64$  m/s, the combustion efficiency increased and reached a maximum at  $v = 0.64$  m/s. When  $u_w > 0.64$  m/s, the combustion efficiency was gradually reduced, ultimately nearly stabilizing, although fluctuations could still be observed. Fig. 9 shows the relationship between combustion efficiency  $\eta$  and  $Re_w^2/Gr_f$ . The dotted area in Fig. 9 showed that the combustion efficiency is higher when  $0.1 \leq Re_w^2/Gr_f \leq 10$ , combustion is at a mixed convection stage and the combustion efficiency  $\eta$  values are higher but fluctuated. When  $Re_w^2/Gr_f > 10$ , the combustion efficiency is reduced and remains stable at a lower value.

261

### 3.4. Relationship between flame-oscillation frequency and combustion efficiency

262

263

264

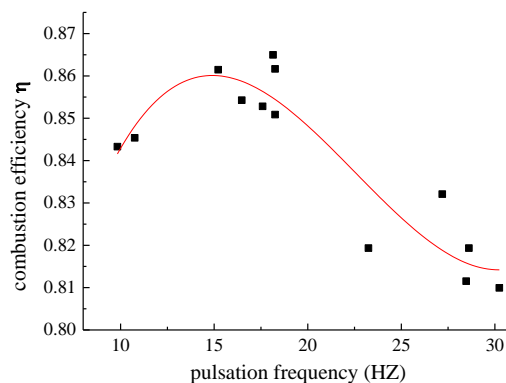
265

266

267

268

The oscillation frequency and combustion efficiency of the flame were both related to the range of different  $Re_w^2/Gr_f$  from the analysis before. The relationship between oscillation frequency and efficiency can be used to visually observe through the oscillation frequency of the flame image (feel from the human eyes) to estimate combustion efficiency. This not only enriched the study of combustion characteristics under the cross wind, but also the oscillation frequency characteristics applied to diagnosis the combustion process. Fig.10 shows a flame-oscillation frequency and combustion efficiency diagram, which were put together for ease comparison.



269

270

Fig.10 Relationship between combustion efficiency and flame oscillation frequency

271

Fig.10 shows that high combustion efficiency concentrated in a range whose flame-oscillation

272 frequency is in 15 Hz - 18 Hz, and relating to the mixing combustion stage, *i.e.*,  $0.1 \leq Re_w^2/Gr_f \leq 10$ ;  
273 the efficiency value was not below 85% in this case. A possible reason is that the shear layer vortex  
274 formed by the interaction between gas and the flame make the fuel and air has been fully mixed, thus  
275 intensifying the combustion and increasing combustion efficiency. When the wind speed was small,  
276 the excess air coefficient was not sufficient to support complete combustion. When forced convection  
277 dominated, even if the amount of oxygen was sufficient, a large amount of cold air would remove the  
278 heat to reduce the flame burning temperature, which will lead to lower combustion efficiency.  
279 According to the experimental image of Fig. 2, it becomes clear that the visible area of the flame  
280 image increased and the combustion efficiency increased during the mixing stage ( $0.44 < u_w < 1.68$   
281 m/s), which can also be proven the high combustion efficiency is in a certain oscillation frequency  
282 range. Only keep the flame-oscillation frequency in 15 Hz-18 Hz, it may ensure combustion efficiency  
283 in right way.

#### 284 4. Conclusions

285 Turbulent flame-oscillation frequency and combustion efficiency are the important parameters in  
286 combustion. Based on the results of wind tunnel experiment and combined the flame sequence image  
287 using a high-speed video and the treatment of MATLAB, the flame-oscillation frequency and  
288 combustion efficiency of 120 mm  $\times$  50 mm  $\times$  50 mm oil pool flames under the action of cross wind  
289 were studied. The following conclusions were drawn:

290 (1) For wind speed of  $0 < u_w < 0.44$  m/s,  $Re_w^2/Gr_f < 0.1$ , the flame was mainly affected by the  
291 buoyancy in the vertical direction. The influence of cross sweeping wind on the flame was dominated  
292 by  $u_w > 1.68$  m/s,  $Re_w^2/Gr_f > 10$  and the mid interval was a mixed phase. In the experimental wind  
293 speed range, with the increase of wind speed, flame-oscillation frequency first increased, then  
294 decreased, and then increased again.

295 (2) With increasing lateral wind speed, the trend of combustion efficiency first increased and then  
296 decreases, reaching a maximum at  $u_w = 0.64$  m/s. When  $0.1 \leq Re_w^2/Gr_f \leq 10$ , the combustion was  
297 in a mixed convection stage where the combustion efficiency fluctuated, but the values are higher. It  
298 was possible to judge the combustion efficiency by observing the fluctuation characteristics of the  
299 flame image.

300 (3) During the mixing stage, the combustion efficiency was higher in the range of turbulent  
301 oscillation frequency of 15 Hz-18 Hz, the combustion efficiency may ensure not below 85% in this  
302 case.

#### 303 Acknowledgments

304 This work was funded by the Natural Science Foundation of Guangdong Province in China  
305 (S2013010016748) and Guangdong Province Key Laboratory of Efficient and Clean Energy  
306 Utilization (2013A061401005), South China University of Technology.

## Nomenclature

$g$  –gravitational acceleration,  $m/s^2$

$Gr_f$  –Grashof number of flame( $=g\alpha_v\Delta T l_w^3/\nu_f^2$ )

$l_w$  –equivalent diameter of the cross section of the wind tunnel, m

$l_f$  –equivalent diameter of the oil sump, m

$R$  –jet-to crossflow momentum flux ratio( $=\rho_j u_j^2/\rho_w u_w^2$ )

$Re_w$  –crosswind Reynolds number( $=u_w l_w/\nu_w$ )

$T_f$  –average temperature of the flame plume, K

$T_\infty$  – ambient temperature, K

$u_w$  –crossflow velocity, m/s

$\nu_f$  –kinematic viscosity of flame plume at average temperature,  $m^2/s$

$\nu_w$  –kinematic viscosity of air,  $m^2/s$

$\alpha_v$  –volume expansion coefficient

307

## 308 References

309 [1] Xiong Yuan, Park Dae Geun, Cha Min Suk, et al. Effect of buoyancy on dynamical responses of  
310 co-flow diffusion flame under low-frequency alternating current. *Combustion Science and*  
311 *Technology*, 190(2018), 10:1832-1849. DOI:10.1080/00102202.2018.1474209

312 [2] Chen Ting, Guo Xiao, Jia Ji, Xiao Jinghua. Frequency and Phase Characteristics of Candle Flame  
313 Oscillation. *Scientific Reports*, 2019, 9:1-13. DOI: 10.1038/s41598-018-36754-w

314 [3] Zukoski E. E., Cetegen B. M., Kubota T.. Visible structure of buoyant diffusion flames. *Symposium*  
315 *on Combustion*, 20(1985), 1: 361-366. DOI:10.1016/S0082-0784(85)80522-1

316 [4] Cetegen, Baki M., Tarek A.. Experiments on the periodic instability of buoyant plumes and pool  
317 fires. *Combustion & Flame*, 93(1993), 1, pp.157-184. DOI:10.1016/0010-2180(93)90090-P

318 [5] Arzler F et al. Burning rates and flame oscillations in globally homogeneous two-phase mixtures.  
319 *Combustion Science and Technology*, (2006), 178, pp.2177-2198. DOI: 10.1080/00102200600626074

320 [6] Kelso R. M., Lim T. T., Perry A. E.. An experimental study of round jets in cross-flow. *Journal of*  
321 *Fluid Mechanics*, 306(1996), pp.111-144. DOI: 10.1017/S0022112096001255

322 [7] Fric, T. F., Roshko A.. Vortical structure in the wake of a transverse jet. *Journal of Fluid Mechanics*,  
323 279(1994), pp.1-47. DOI: 10.1017/S0022112094003800

324 [8] Tsue, Mitsuhiro, Toshikazu Kadota, Michikata Kono. Temperature and velocity fluctuations of a jet  
325 diffusion flame in a cross-flow. *Proceedings of the Combustion Institute*,  
326 29(2002), pp.1937-1942. DOI: 10.1016/S1540-7489(02)80235-8

- 327 [9]Bourguignon, E., Johnson M. R., Kostiuk L. W.. The use of a closed-loop wind tunnel for  
328 measuring the combustion efficiency of flames in a cross flow. *Combustion & Flame*,  
329 119(1999),3,pp.319-334. DOI: 10.1016/S0010-2180(99)00068-1
- 330 [10]Gogolek P. E. G, Hayden A. C. S. Efficiency of Flare Flames in Turbulent cross wind. American  
331 Flame Research Committee, 2010.
- 332 [11]Johnson, M. R., Kostiuk L. W.. Efficiencies of low-momentum jet diffusion flames in crosswinds.  
333 *Combustion & Flame*, 123, (2000),1–2,pp.189-200.DOI: 10.1016/S0010-2180(00)00151-6
- 334 [12]Johnson, M. R., Kostiuk L. W..A parametric model for the efficiency of a flare in crosswind.  
335 Proceedings of the Combustion Institute, 29, (2002), 2,pp.1943-1950.  
336 DOI: 10.1016/S1540-7489(02)80236-X
- 337 [13]Fang, Jun, et al. Momentum and buoyancy-driven laminar methane diffusion flame shapes and  
338 radiation characteristics at sub-atmospheric pressures. *Fuel*, 163,(2016),pp.295-303.  
339 DOI: 10.1016/j.fuel.2015.09.068
- 340 [14]Ping Ping, He, Xu, Kong Depeng.An experimental investigation of burning rate and flame tilt of  
341 the boilover fire under cross air flows. *Applied thermal engineering*,133,(2018),pp.501-511.  
342 DOI: 10.1016/j.applthermaleng.2018.01.066
- 343 [15]Malalasekera W. M. G., Versteeg H. K., Gilchrist K.. Review of research and experimental study  
344 on the pulsation of buoyant diffusion flames and pool fires[J]. *Fire & Materials*, 20(1996),6,  
345 pp.261-271.DIO:10.1002/(SICI)1099-1018(199611)20:6<261::AID-FAM578>3.0.CO;2-M
- 346 [16]Lou Bo, Qiu Yonghai, Xu jianhong. Characteristics of diffusion flames with accelerated motion.  
347 *Thermal Science*, 20,(2016),6,pp.2113-2124.DOI: 10.2298/TSCI150413180L
- 348 [17]Hu Longhua, et al. Flame size and volumetric heat release rate of turbulent buoyant jet diffusion  
349 flames in normal- and a sub-atmospheric pressure[J]. *Fuel*, 150(2015),pp.278-287.  
350 DOI: 10.1016/j.fuel.2015.01.081
- 351 [18]Gollahalli S. R., T. A.. Brzustowski, H. F. Sullivan. Characteristics of a turbulent propane  
352 diffusion flame in a cross-wind. *Transactions- Canadian Society for Mechanical Engineering*,  
353 3(1975),4,pp. 205-214.
- 354 [19]Maughan J. R.,F. P.. Experiments on mixed convection heat transfer for airflow in a horizontal and  
355 inclined channel. *International Journal of Heat & Mass Transfer*, 30(1987),7,pp.1307-1318.  
356 DOI: 10.1016/0017-9310(87)90163-3
- 357 [20]Fang Jun, et al. Influence of low air pressure on combustion characteristics and flame pulsation  
358 frequency of pool fires. *Fuel*, 90(2011),8,pp.2760-2766.DOI: 10.1016/j.fuel.2011.03.035
- 359 [21]Darabkhani, H. Gohari, et al. Impact of co-flow air on buoyant diffusion flames flicker. *Energy*  
360 *Conversion & Management*,52(2011),8,pp.2996-3003.DOI: 10.1016/j.enconman.2011.04.011
- 361 [22] Hu Longhua, et al. A wind tunnel experimental study on burning rate enhancement behavior of  
362 gasoline pool fires by cross air flow. *Combustion & Flame*, 158(2011),3,pp.586-591.  
363 DOI: 10.1016/j.combustflame.2010.10.013

364 [23]Tao Changfa. The study of combustion characteristic and heat transfer mechanism of alcohol pool  
365 fire under oblique air flow(in Chinese). Ph. D. thesis, University of science and technology of china,  
366 Hefei, China,2013